JOURNAL OF AGRICULTURAL AND FOOD CHEMISTRY

ARTICLE

pubs.acs.org/JAFC

Bound Fatty Acids Modulate the Sensitivity of Bovine β-Lactoglobulin to Chemical and Physical Denaturation

Alberto Barbiroli,[†] Francesco Bonomi,[†] Pasquale Ferranti,[§] Dimitrios Fessas,[‡] Antonella Nasi,[§] Patrizia Rasmussen,[†] and Stefania Iametti*[,†]

[†]Section of Biochemistry, DISMA, and [‡]Calorimetry Lab, DISTAM, Università degli Studi di Milano, Via Celoria 2, 20133 Milan, Italy

[§]DSA, University of Naples "Federico II", 80055 Portici, Italy

Supporting Information

ABSTRACT: Fatty acids are the natural ligands associated with the bovine milk lipocalin, β-lactoglobulin (BLG), and were identified by means of mass spectrometry. The naturally bound ligands were found to contribute to the stability of the proteins toward denaturation by both temperature and chaotropes. To assess the nature of the structural regions involved in this stabilization, the thermodynamic and kinetic aspects of the stability of various structural regions of the proteins were studied in the presence of bound palmitate, which is the most abundant natural ligand. Binding of a single palmitate molecule was found to affect not only the stability of the calyx region, where palmitate is bound, but also that of the region at the hydrophobic interface between the barrel itself and the long helix in the protein structure, where the thiol group of Cys121 is buried. This region is known to be essential for the stability of the BLG dimer and is relevant to the generation of "reactive monomers" that are involved in covalent and noncovalent polymerization of BLG and in the formation of covalent adducts with other milk proteins.

KEYWORDS: β-lactoglobulin, fatty acids, folding stability, heat denaturation

INTRODUCTION

The globular protein β-lactoglobulin (BLG) is found in the whey fraction of the milk of many mammals, where its function is still not clearly understood.[1,2] The crystal structure of BLG reveals a marked similarity with the plasma retinol binding protein and the odorant binding protein, which all belong to the lipocalin superfamily.[2−5] All of these proteins share the same structural elements and are characterized by a β-barreled central cavity, mainly responsible for the binding of hydrophobes, and by additional elements of secondary structure that often act as determinants of their biological function.

In the case of BLG, these additional structural features are represented by a sizable α-helix region, which is involved in the formation of a noncovalent dimer at neutral pH by establishing intermonomer hydrophobic contacts and electrostatic interactions (Figure 1). The helix face opposing the dimerization interface forms a hydrophobic groove with respect to the β-barrel. The lone free thiol of Cys121 is buried in this groove, and its exposure has been correlated to dimer dissociation in the earliest phases of reversible events in the physical denaturation of BLG,[6−8] as well as to disulfide exchange events in the irreversible phases of physical[9] and chemical[10] denaturation, which are of interest for food processing.

Denaturation of BLG by physical means is a complex phenomenon that occurs through a series of intermediate steps, the rates and/or equilibria of which depend on the treatment conditions, on the protein concentration, and on the interaction with other components when complex systems such as milk and whey are considered. Most of the steps occurring below a given intensity threshold of physical treatment (temperatures below 60−65 °C or pressures below 400 MPa[11,12]) are fully reversible in solutions of the pure protein at neutral pH. Transient BLG conformers are formed by either physical treatment, and the properties of these conformers have been investigated in some detail,[6,7,11,13−15] also by using limited proteolysis approaches.[16]

In view of their practical relevance, the thermodynamics and the kinetics of the various steps in the physical denaturation of BLG have been investigated extensively. By combining various experimental approaches, two independent energetic domains were found to be sequentially and independently altered as temperature increases: a first, low-temperature domain was associated with modifications in the helix−barrel hydrophobic contacts,[8] whereas modifications at higher temperatures have been interpreted as due to alterations affecting the hydrophobic cavity outlined by the β-barrel structure.[6]

Modifications leading to transiently or permanently modified structures of BLG are expected to affect the ligand binding properties of the protein. In turn, as observed for many other proteins, the presence of protein-bound ligands is expected to affect the stability of the various structural regions on proteins involved in their recognition. Also, ligand binding or dissociation from "flexible" regions of protein structure is often involved in triggering responses of physiological relevance, as well as in fundamental processes such as transport or cofactor uptake.

A number of studies involving likely physiological ligands of BLG proved that BLG is capable of binding different hydrophobic molecules,[17,18] some of them simultaneously,[19] and that ligands having some hydrophobic "tail", such as fatty acids and retinol, bind to the calyx region of the molecule.[20] BLG retains its

Received: February 2, 2011
Revised: April 19, 2011
Accepted: April 20, 2011
Published: April 20, 2011

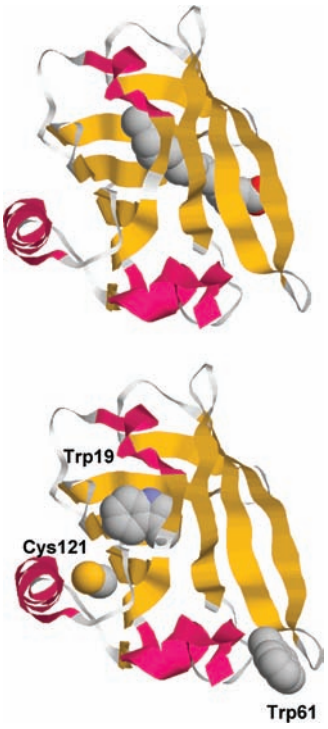

Figure 1. Cartoons depicting some structural features of the BLG monomer: (top) palmitate bound to the β-barrel calyx shown in spacefilling, CPK coloring; (bottom, same orientation as top) side chains of amino acid residues relevant to this study. Backbone is given as ribbons: helices are in red, β-strands in yellow. Graphs were generated by using RASMOL,[37] from coordinates deposited in file 1GXA[20] in the Protein Data Bank.

binding capacity toward fatty acids over a wide pH range[17] and even at very high concentrations of chemical denaturants.[21] However, little is known about the stability of these interactions in the case of thermal treatments and whether these interactions affect the stability of the protein as a whole rather than limited regions relevant to its treatment-dependent modifications. Because BLG is likely present in milk and in milk-derived ingredients as a mixture of complexes with various (but yet poorly defined) ligands, ligand-dependent stabilization of structural features affecting its behavior and reactivity may be of practical relevance.

For these reasons, in this work we assessed at first the nature of the ligands associated with BLG when isolated from milk, and then we studied how this association affects the chemical and physical denaturation of the protein. Having confirmed a ligand-dependent stabilization of the "as-isolated" protein structure of BLG toward denaturants, we used palmitate-saturated BLG to carry out a detailed structural, thermodynamic, and kinetic characterization of ligand-dependent stabilization.

MATERIALS AND METHODS

Protein and Chemicals. BLG was purified from cow's milk according to the literature[4] and defatted when indicated by stripping the natural ligands on a Lipidex-1000 column as in ref 22. Aliquots of the defatted protein in 50 mM phosphate buffer, pH 6.8, were dialyzed in an Amicon ultrafiltration cell and concentrated by using a Centricon YM5 membrane (Amicon). Unless otherwise specified, 50 mM phosphate buffer, pH 6.8, was the buffer used in all of these studies. Palmitate-saturated BLG was prepared by adding to the defatted BLG (1 mg/mL) a 20-fold molar excess of palmitic acid (from a stock solution 50 mM in ethanol). After 16 h of incubation at room temperature, palmitate-saturated BLG was separated from the unbound palmitic acid by ultrafiltration in a Centricon YM5 device (Amicon).

Analytical and Spectroscopic Measurements. Circular dichroism (CD) studies were carried out on a Jasco J810 spectropolarimeter. Spectra of a 2 mg/mL protein solution were recorded in a 1 cm path length cell and analyzed by means of Jasco J800 software. In temperature ramp experiments, the temperature was increased from 20 to 95 °C at 0.5 °C/min. T_m values were calculated from the first derivative of the recorded traces.

Spectrofluorometric studies were carried out in a Perkin-Elmer LS50 instrument. Tryptophan emission spectra were collected by using λ_{ex} = 298 nm. Surface hydrophobic properties of the proteins were analyzed by titration with the fluorescent probe 1,8-anilinonaphthalenesulfonate (ANS), at λ_{ex} = 390 nm and λ_{em} = 480 nm. Accessible protein thiols were detected spectrophotometrically in a Perkin-Elmer Lambda S2 instrument by using 5,5′-dithiobis(2-nitrobenzoic acid) (DTNB).[23]

Denaturation kinetics were monitored by diluting BLG solutions with urea solutions of appropriate concentration. The volume ratio BLG/urea was 1/5, and the final protein concentration was 1 mg/mL. Thiol exposure was measured by adding 0.2 mM DTNB to the urea solution and monitoring the absorbance increase at 412 nm following BLG addition by manual mixing techniques.[6,10]

Stopped-flow CD and fluorescence measurements were carried out at 25 °C by using a stopped-flow apparatus (BioLogic, France; model SFM 20) with a four-optical surface and 2 mm path length quartz cell. The stopped-flow apparatus was attached to a J810 spectropolarimeter operating at 292 nm and fitted with a fluorescent detector placed orthogonally to the CD light beam. This experimental setup allowed simultaneous recording of the sample fluorescence (emission at 345 nm) and of changes in ellipticity at 292 nm. In all cases, kinetics were analyzed by using standard software tools.

Analysis of Unfolding Equilibria. Chaotrope unfolding curves were analyzed using a two-state mechanism. Unfolding curves for the N↔U transition were normalized to the apparent fraction of the unfolded form,[24] and data were analyzed by assuming the free energy of unfolding or refolding, $\Delta G°$, to be linearly dependent on the urea concentration (denoted here by C):[24]

$$\Delta G° = \Delta G°_w - mC = m(C_m - C) \quad (1)$$

$\Delta G°_w$ and $\Delta G°$ represent the free energy of unfolding or refolding in the absence and presence of urea, respectively; C_m is the midpoint concentration of urea, that is, at K = 1 for unfolding or refolding equilibria; and m stands for the slope of the unfolding or refolding curve at C_m. A least-squares curve fitting analysis was used to calculate the values of $\Delta G°_w$, m, and C_m by a software routine.

Differential Scanning Calorimetry (DSC). Calorimetric measurements were carried out on solutions with a protein concentration of 10 mg/mL in 50 mM phosphate buffer, pH 6.8, with a third-generation Setaram Micro-DSC apparatus at 0.5 °C/min scan rate. Data were analyzed by means of the software THESEUS.[25] The excess molar heat capacity $\langle \Delta C_p \rangle$ or $C_p^E(T)$, that is, the difference between the apparent molar heat capacity $C_p(T)$ of the sample and the molar heat capacity of the "native state", $C_{p,N}(T)$, was recorded across the scanned temperature range. Details on the raw data treatment methods, (baselines scaling, etc.) were reported elsewhere.[8] The heat capacity drop across the signal, $\Delta_d C_p$, was affected by a rather large error (about 8 ± 4 kJ mol^{-1}) and was therefore not taken into account in the present work.

The theoretical models used to fit the experimental data were tested through the nonlinear Levenberg−Marquardt method.[26] The best fit was obtained by using the same model as in the case of free BLG,[8] that is, by assuming that two protein domains could undergo denaturation

independently, with an equilibrium mechanism followed by an irreversible step.

$$N_i \leftrightarrow D_i \rightarrow I_i \quad (i = 1, 2) \tag{2}$$

For each domain the excess heat capacity can be given by the equation[27]

$$C_{p\,i}^{E} = \frac{K_i \Delta_d H_i^{\circ}}{(K_i + 1)^2}\left(\frac{k_i}{\beta} + \frac{\Delta_d H_i^{\circ}}{RT^2}\right)\exp\left\{-\frac{1}{\beta}\int_{T_0}^{T}\frac{k_i K_i}{K_i + 1}\,dT\right\} \tag{3}$$

where β is the scanning rate (K min^{-1}).

K_i is given by eq 4

$$K_i(T) = \exp\left\{-\frac{\Delta_d H_i^{\circ}}{R}\left(\frac{1}{T} - \frac{1}{T_d^i}\right)\right\} \tag{4}$$

where $\Delta_d H_i^{\circ}$ and T_d^i are the standard denaturation enthalpy and denaturation temperature, respectively, for each independent domain. Both a zero reaction enthalpy[8] and first-order kinetics were assumed for the irreversible step, with a kinetic constant obeying the Arrhenius equation:

$$\kappa_i = \exp\left(-\frac{E_{a,i}}{R}\left(\frac{1}{T} - \frac{1}{T_i^*}\right)\right) \tag{5}$$

$E_{a,i}$ here is the activation energy of the irreversible step ($D_i \rightarrow I_i$), and T_i^* is the temperature at which the apparent kinetic constant k_i = 1 min^{-1}. The overall $C_p^E(T)$ therefore is

$$C_p^E(T) = \sum_{i=1}^{n} C_{p\,i}^{E}(T) \tag{6}$$

Mass Spectrometry and GC-MS. *Mass Spectrometry of BLG Adducts.* A Q-TOF Ultima mass spectrometer (Waters, U.K.) was used in positive ion mode in all of the experiments. Ten microliter aliquots of reaction mixture were introduced through a Rheodyne external loop injector into the ion source at a flow rate set to 1 μL/min by a Phoenix 20 CU HPLC pump driving a gastight syringe connected to the instrument capillary. To obtain maximum signals for the ions of the putative molecular complex, a solution of 5% acetonitrile in 10 mM ammonium hydrogen carbonate, pH 7.0, was used. Different conditions of orifice voltage (20−80 V) and temperature (40−100 °C) were tested, and a declustering potential of 40 V and a source temperature of 60 °C were chosen because under these particular conditions no fragmentation was observed and optimum sensitivity for the adduct peaks was attained. Spraying was achieved by charging the probe at 3.6 kV using nitrogen as the nebulizing gas. Calibration of the mass scale was performed using the multiple charged ions of horse heart myoglobin from a separate sample introduction in positive ion mode. Full-scan mass spectra were generated in continuous data acquisition mode. The spectra reported are an average of three scans from m/z 800 to 2200 (scan rate = 10 s/scan). Quantitative analysis of components was performed by integration of the multiple-charge ions relative to each species.

GC-MS Analysis of Ligands. For GC-MS analysis, organic extracts from BLG samples were dried, redissolved in hexane, and transmethylated by addition of 0.1 mL of saturated methanolic KOH. A sample aliquot (1 μL) was injected in an HP6890 gas chromatograph (Agilent Technologies, Santa Clara, CA) coupled to a 5973N quadrupole mass spectrometer (Agilent) operating in positive electron impact ion mode. The gas chromatograph was equipped with an HP-5 ms capillary column (30 m × 0.25 mm i.d.), and the carrier gas was helium. The GC oven temperature was programmed from 40 °C (hold for 7 min) to 180 °C at 5 °C/min. The masses were scanned over an m/z range of 45−350 amu.

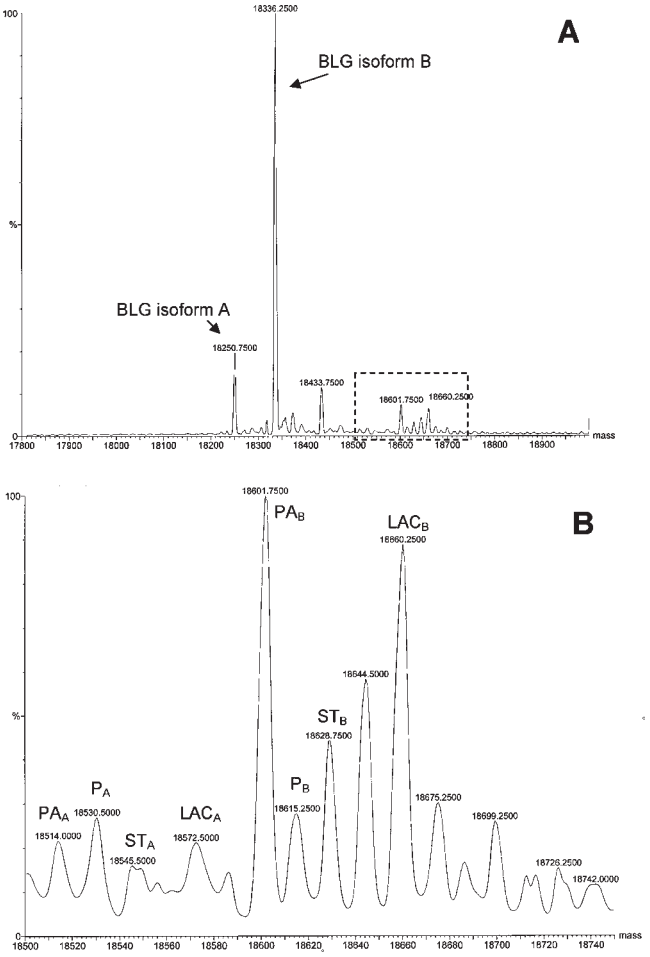

Figure 2. MS identification of natural ligands in BLG: (A) ESI-MS spectra of as-isolated BLG (before Lipidex treatment) (the dashed box points out the region of the complex between BLG and the natural ligands); (B) magnification of the box in panel A (naturally occurring complexes between isoforms A and B of BLG (indicated by subscripts) and palmitic acid (PA), stearic acid (ST), lactose (LAC), and phosphate (P)).

The NIST library and/or comparison with spectra and retention times of standards was used for the identification of compounds. Quantitative analysis was carried out through calibration in matrix in the range of verified linearity; multiple replicates (n = 3−6) of the samples were analyzed, using a 1 mg/mL solution of methyl nonadecanoate as internal standard.

RESULTS AND DISCUSSION

Characterization of Naturally Occurring BLG Ligands and of Their Effects on Protein Stability. The nature of ligands remaining bound to minimally treated, as-isolated BLG was investigated by two different methods, namely, ESI mass spectrometry of the protein−ligand complexes and GC-MS analysis of the lipid components remaining bound to the Lipidex resin used for obtaining the ligand-free form of the protein. The ESI-MS spectra of the as-isolated BLG are shown in Figure 2 and indicate that this preparation contained ligand-free BLG along with bimolecular complexes between BLG and individual heterogeneous ligands. Saturated fatty acids were the most common ligands, and palmitate was the most abundant among them.

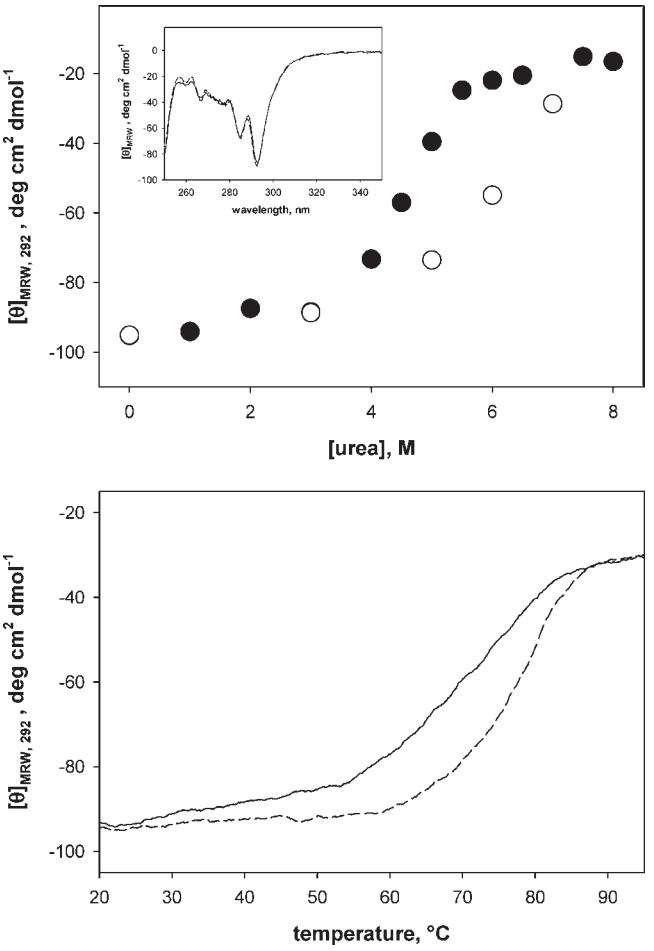

Figure 3. Naturally occurring ligands stabilize BLG against thermal and urea denaturation: (top) unfolding titration curves, monitored by circular dichroism at 292 nm, of the ligand-free (solid symbols) and as-isolated (open symbols) BLG as a function of urea concentration ((inset) near-UV CD spectra of as-isolated (dashed line) and Lipidex-treated, ligand-free BLG (solid line)); (bottom) temperature ramp monitored by circular dichroism at 292 nm for the ligand-free (solid line) and as-isolated (dashed line) BLG.

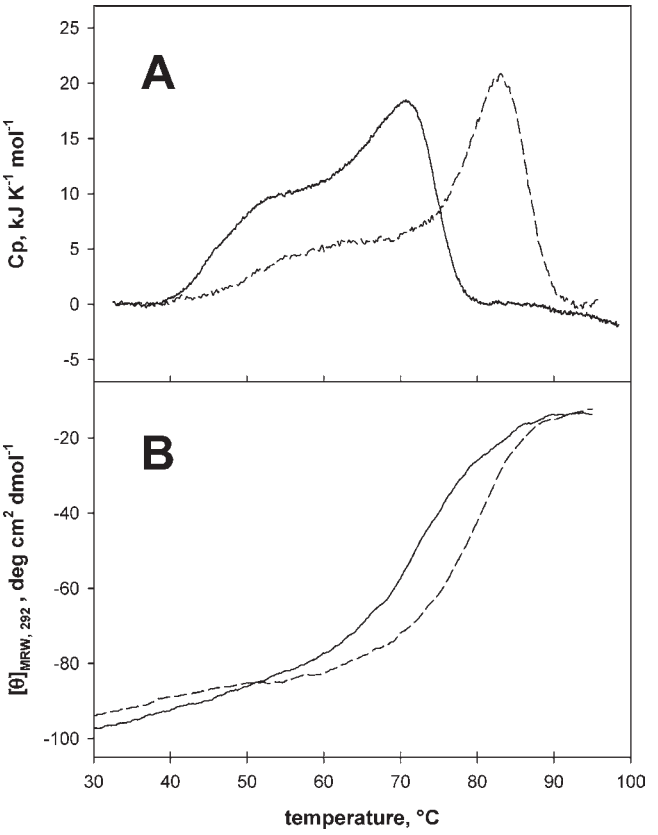

Figure 4. Thermal denaturation of ligand-free and palmitate-saturated BLG: DSC traces (A) and variation of CD signal as a function of temperature (B) for ligand-free (solid line) and palmitate-saturated (dashed line) BLG. The DSC trace for ligand-free BLG was taken from ref 8.

These hydrophobic ligands were completely removed after Lipidex treatment as confirmed by ESI-MS spectra of the Lipidex-treated protein (not shown). GC-MS analysis of the nonpolar fractions bound to the Lipidex column, eluted with appropriate organic solvents (Figure 1S of the Supporting Information) showed the presence of various saturated fatty acids and of oleic acid. Palmitic acid was the most abundant species, confirming the information provided by MS studies on the as-isolated protein.

The presence of naturally occurring ligands did not alter the spectral features of BLG related to its tertiary structure (Figure 3, inset), confirming a number of previous reports.[21,22] However, as shown in Figure 3, naturally occurring ligands greatly influenced the sensitivity of these spectral features to chemical and physical denaturants. Ligand-free BLG was more sensitive to urea-induced loss of tertiary structure than as-isolated BLG. The C_m for urea-induced loss of CD-detectable tertiary structure, calculated from urea titrations such as those in Figure 3, was 5.6 M for as-isolated BLG and decreased to 4 M after the removal of the naturally occurring ligands. As also shown in Figure 3, progressive heating experiments gave a T_m for the loss of the near-UV CD signal associated with native tertiary structure in as-isolated BLG of 78 °C, that is, ∼6 °C higher than the value measured for ligand-free BLG.

Given the presence of multiple forms of BLG in our as-isolated material, differing as to the amount and the nature of the associated ligand, we prepared a palmitate-saturated protein by exposing ligand-free BLG to saturating amounts of palmitate. This protein−ligand complex was used to assess which structural regions are relevant to ligand-dependent stabilization.

Structural Features of Ligand-free and Palmitate-Saturated BLG. The procedure used for preparing palmitate-saturated BLG gave a protein containing >90% of a species in which one palmitate residue was bound per BLG monomer. ESI-MS characterization of the palmitate-saturated BLG ruled out the possibility that more than one palmitate molecule was bound per BLG monomer, in agreement with previous crystallographic evidence[20] and with data obtained in ^{19}F NMR and MS studies on complexes of BLG with 2-fluoropalmitate.[22]

As discussed in the previous section, and as shown in a further section, the near-UV CD spectra and the tryptophan emission fluorescence spectra of native BLG were only very marginally affected by bound palmitate.[28] We carried out ANS titration studies to assess whether bound palmitate caused any rearrangement in the surface hydrophobicity of BLG.[29,30] Whereas the number of ANS-binding surface sites was unaffected by the presence of palmitate, we noted that the palmitate-saturated

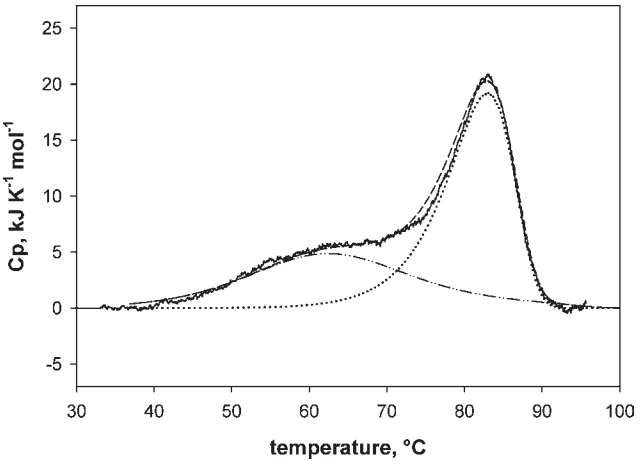

Figure 5. Best fit of the DSC trace of palmitate-saturated BLG. The experimental tracing is given as a solid line. Dash-dot-dotted and dotted lines correspond to the contributions attributed to the first and second energetic domains, respectively. The overall fit is given as the dashed line.

protein had a lower affinity for ANS. The dissociation constant for the supposedly bimolecular ANS−BLG complex[10,29,30] increased about 25% in palmitate saturated-BLG (from 57 to 72 μM).

Bound Palmitic Acid and Stability toward Denaturants: Kinetic and Thermodynamic Aspects. Palmitate-saturated BLG was characterized for its thermodynamic stability toward chemical and physical denaturants by following spectroscopic changes (near-UV CD and tryptophan fluorescence) in the course of urea titration and temperature ramp experiments. The signature spectroscopic features of the protein were also used to assess the reversibility of changes induced by either type of denaturants. Furthermore, the thermal stability was also assessed by DSC.

The increased thermal stability of palmitate-saturated BLG with respect to the free BLG is evident when one considers the DSC traces presented in Figure 4A, where the presence of palmitate influences the stability of both the energetic domains recognized in previous studies and associated with defined regions of the protein structure[8] and increases the denaturation temperature.

To quantify such qualitative evidence, the DSC trace of palmitate-saturated BLG was fitted using the same denaturation model proposed for palmitate-free BLG.[8] The fitting results are presented in Figure 5, and the best-fit parameters are reported in Table 1. The T_d of the second and most evident energetic domain (associated mainly with the β-barrel region of the protein[8]) increases more than 10 °C in the presence of palmitate (from 70.5 to 83.5 °C), with no significant variation of the denaturation enthalpy. Palmitate also stabilizes the first energetic domain, associated mainly with the interactions between the C-terminal long helix and the β-barrel region,[8] by shifting upward its denaturation temperature (from 55 to 63 °C) with a concomitant broadening of the associated signal and a decrease of the associated denaturation enthalpy. According to these pieces of evidence, it may be concluded that the stabilization of both domains by bound palmitate is due to entropic factors.

Furthermore, both the DSC profiles and the kinetic data in Table 1 show that the presence of palmitate does not affect substantially the irreversible step that leads to denaturation of the

Table 1. Best-Fit Parameters for the DSC Tracing Obtained for Free BLG and Palmitate-Saturated BLG[a]

	$\Delta_dH°$ (kJ mol^{-1})	T_d (°C)	E_a (kJ mol^{-1})	T^* (°C)
BLG				
first domain	180 ± 10	55.0 ± 0.3	250 ± 15	T_d + 50.0 ± 0.5
second domain	205 ± 10	70.5 ± 0.3	240 ± 15	T_d + 27.7 ± 0.5
BLG + palmitate				
first domain	135 ± 10	63.0 ± 0.3	250 ± 15	T_d + 55.0 ± 0.5
second domain	220 ± 10	83.5 ± 0.3	240 ± 15	T_d + 27.0 ± 0.5

[a] The fit parameters for palmitate-free BLG (taken from ref 8) are compared with the fit parameters calculated for a palmitate-saturated BLG from the data in Figures 3 and 4, according to a model including an aggregation step and assuming two independent energetic domains.

second energetic domain (if not for an overall shift of the aggregation temperature range), but does affect that of the first domain (resulting in a higher value of T^*, which represents an estimate of the kinetic component of the process).

The overall palmitate stabilization effect was also confirmed spectroscopically. Although these experiments are not directly comparable with the DSC traces because of the different protein concentrations of the samples (that influence the T_m due to the irreversible aggregation step, which is, obviously, a concentration-dependent event), they confirm that the presence of palmitate increases the denaturation temperature.

As shown in Figure 4B, progressive heating of either protein from 20 to 95 at 0.5 °C/min resulted in irreversible loss of most of the near-UV CD features of BLG, in particular in the 292 nm region, as reported elsewhere.[8] However, the midpoint temperature for the CD-detectable transition is significantly higher in the palmitate-saturated (81 °C) than in the ligand-free BLG (72 °C) or in as-isolated BLG in the presence of naturally occurring ligands (78 °C, see Figure 3).

As already pointed out in ref 8 and as made evident from the comparison of panels A and B in Figure 4, the second, high-temperature domain corresponds to loss of tertiary structure in the central barrel, which harbors the spectroscopically relevant Trp19 residue (see Figure 1). The first, low-temperature thermal transition has been associated with structural changes in the helical region involved in dimerization and in the shielding of the Cys121 thiol group.[8] The fact that the palmitate molecule bound within the barrel cavity[20,31] exerts a structural protection on this region as well appears to be worth investigating, in terms of the reported significance of the overall structural flexibility of this protein with respect to its ligand binding properties.[15]

Despite the practical relevance of the different temperature sensitivities of the two BLG forms, the irreversibility of the temperature-induced modifications beyond a given temperature threshold (~65 °C at the pH and protein concentrations used in our studies) makes it difficult to carry out a quantitative analysis of the temperature effects.

On the other hand, we found that the structural modifications induced by urea were almost completely and promptly reversible, at least in terms of the recovery of spectroscopic signals, following a 10-fold dilution in plain buffer of the urea-treated protein, regardless of the presence/absence of palmitate. This allowed a more thorough thermodynamic analysis of the denaturant effects on both protein forms.

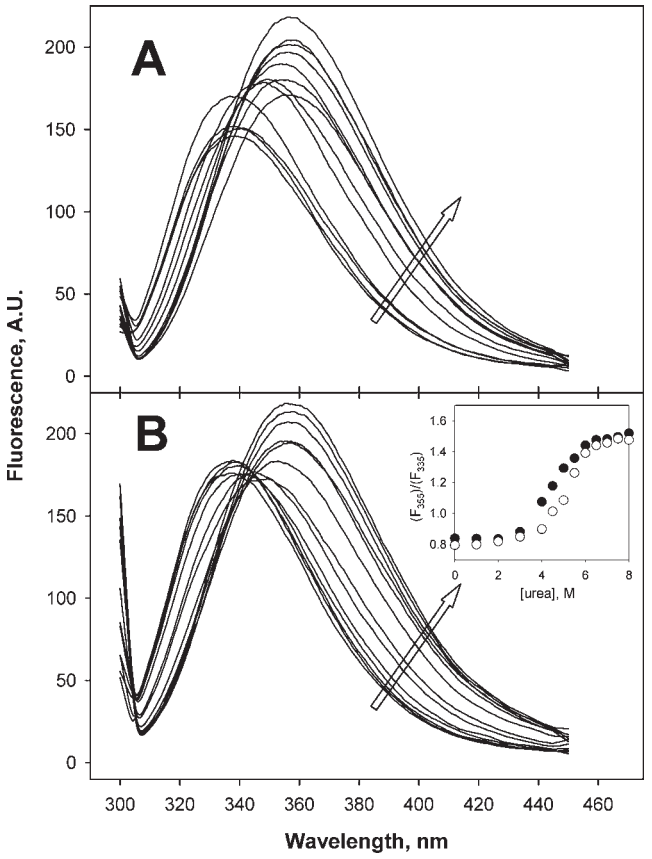

Figure 6. Tryptophan fluorescence emission spectra of ligand-free (A) and palmitate-saturated (B) BLG at various urea concentrations (arrows indicate increasing urea concentration). (Inset) relative fluorescence intensity ($F_{355\ nm}/F_{335\ nm}$) as a function of urea concentration for ligand-free BLG (solid symbols) and palmitate-saturated BLG (open symbols).

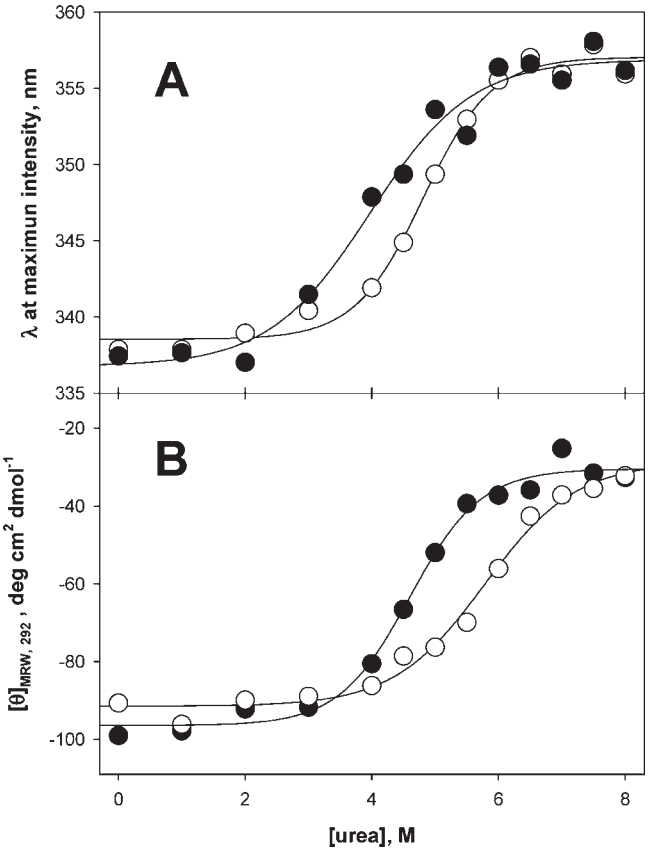

Figure 7. Urea dependence of tertiary structure features in palmitate-saturated (open symbols) and ligand-free (solid symbols) BLG: (A) Trp fluorescence emission signal; (B) intensity of the CD signal at 292 nm.

Changes in the elipticity at 292 nm and in the intensity of protein fluorescence at equilibrium as a function of the urea concentration were used for calculating the thermodynamic parameters for chaotrope denaturation of the various protein forms, as shown in Figures 6 and 7, which are summarized in Table 2. The concentration of urea at denaturation midpoint (C_m) detected with both spectroscopic approaches was higher for the palmitate-saturated BLG. The data presented in Table 2 also indicate that the tryptophan fluorescence is much more sensitive to urea than the tryptophan contribution to the near-UV CD signal. This effect is observed both in ligand-free BLG (4 vs 4.5 M) and in palmitate-saturated BLG (4.8 vs 5.7 M).

However, fluorescence spectra measured at increasing urea concentration in the presence of palmitate (Figure 7) show a pattern of changes that differs from that recorded on ligand-free BLG. However, the emission fluorescence spectra recorded in the presence of palmitate (and the resulting denaturation curve, Figure 7, inset) are consistent with a two-state model, which seemingly also applies to the spectral changes observed in the absence of the ligand.

Variation in the wavelength of Trp fluorescence maximum emission during denaturation of ligand-free BLG is reportedly ascribed to the Try19,[32] which is located at the bottom of the protein β-barrel (see Figure 1). This particular tryptophan residue is well conserved in all of the lipocalins, suggesting that it may play a fundamental role in the folding of this protein family.[33,34] Conversely, contributions to the CD signal are expected to come from both Trp19 and Trp61. Figure 1 shows that this latter residue is located in a surface region close to the pH-sensitive E−F loop "lid" that modulates ligand access (see ref 21 and references cited therein). The surface location and the solvent exposure of Trp61 make unlikely any change in its chemical environment (and thus any marked change in the position of its fluorescence maximum) when the protein structure is altered.

The data in Table 2 also made it evident that, both in the absence and in the presence of palmitate, the chemical environment of the "buried" Trp19 is altered at lower chaotrope concentration than that of the exposed Trp61. However, the palmitate-dependent upward shift in C_m is higher for the CD signal (from 4.5 to 5.7 M urea) than for the fluorescence signal (from 4 to 4.8 M urea). In view of the complexity of this situation, we resorted to a kinetic analysis of the dependence of the rate of the observed changes (and of other structural indicators), as detailed in the following section.

Kinetic Aspects of the Stabilizing Effects of Bound Palmitate. The maximum intensity of the negative CD contribution of the tryptophan residues in BLG is at 292 nm, which is also the maximum for excitation of the Trp fluorescence. This made it possible and convenient to study simultaneously changes in both spectroscopic parameters upon mixing of BLG with urea solutions of various concentration in a stopped-flow cell.

Pseudo-first-order rate constants for spectroscopically detectable changes are listed in Table 3. No changes were detectable at

Table 2. Thermodynamic Parameters for Urea Denaturation of Free and Palmitate-Saturated BLG[a]

	tryptophan fluorescence emission maximum		intensity of tryptophan CD signal in the near-UV region	
	BLG	BLG + palmitate	BLG	BLG + palmitate
$\Delta G°_w$ (kJ mol^{-1})	11.7	14.8	13.9	16.3
C_m (M)	4.0	4.8	4.5	5.7
m (kJ mol^{-1} M^{-1})	2.9	3.1	3.1	2.9

[a] Thermodynamic parameters are calculated from urea titration experiments similar to those reported in Figure 6.

Table 3. Kinetic Parameters for Urea-Induced Unfolding of BLG[a]

	pseudo-first-order rate constant of observed changes (min^{-1})			
	tryptophan fluorescence, emission intensity at 345 nm		intensity of tryptophan near-UV CD signal at 292 nm	
urea (M)	ligand-free	palmitate-saturated	ligand-free	palmitate-saturated
4	4.9 ± 0.2	not observed[b]	not observed[b]	not observed[b]
5	5.2 ± 0.8	1.6 ± 0.2	5.0 ± 0.3	not observed[b]
6	10.8 ± 0.7	0.9 ± 0.1	11.7 ± 0.8	1.8 ± 0.4

[a] Pseudo-first-order rate constants were calculated from semilog plots of the fractional variation of the monitored parameter vs time. These plots were linear for at least two reaction half-times. [b] No detectable changes at these urea concentrations.

urea concentrations below the threshold detected in equilibrium measurements (Figure 7), indicating the absence of kinetic intermediates as for attaining the equilibria depicted in Figures 6 and 7. Rates of urea-induced modification in each spectroscopic parameter were almost identical for ligand-free BLG and decreased significantly when palmitate was bound to the protein. At 6 M urea, at which even the palmitate-bound protein is >60% unfolded, the slowest detectable event is the change in fluorescence of Trp19, being slower than CD changes. This implies that (1) bound palmitate kinetically stabilizes against exposure of buried Trp19 to the solvent and (2) the contribution of Trp61 to the CD spectrum is altered independently of that of Trp19, from both a kinetic and thermodynamic standpoint, because it is faster than changes involving the calyx bottom, although it requires higher urea concentrations.

The lone thiol of Cys121 also provides a convenient marker of structural changes in BLG. This residue is buried in a hydrophobic groove between the long helix and the outside of the β-barrel (Figure 1). At neutral pH, its exposure is the result of movement of the helix away from the barrel, a process that is affected even by the mildest denaturing conditions, regardless of whether physical or chemical agents are used.[10] The Cys121 thiol is known to be involved in disulfide exchange events that eventually lead to the formation of various types of polymeric structures upon physical or chemical denaturation of BLG.[6,9,10] Exposure of thiols in BLG also plays a role in the well-known formation of a mixed disulfide with κ-casein in heat-processed milk, which in turn affects enzymatic curding and cheesemaking.

The rates of exposure of the Cys121 thiol may be monitored by conventional spectrophotometry by using a suitable excess of the common thiol reagent DTNB and were found to increase as an exponential function of urea concentration, as shown in Figure 8. However, rate changes were appreciable at urea concentrations well below the threshold required for the modifications detected by CD and fluorescence studies. This confirms that exposure of the Cys121 thiol and loss of structure in the barrel region are separate events, occurring at independent rates and with a different sensitivity to urea. This is confirmed by the observation that at 4 M urea the structural rearrangement leading to exposure of the Cys121 thiol in ligand-free BLG occurs at 0.297 min^{-1}, a much slower rate than that measured for fluorescence changes (4.9 min^{-1}, Table 1).

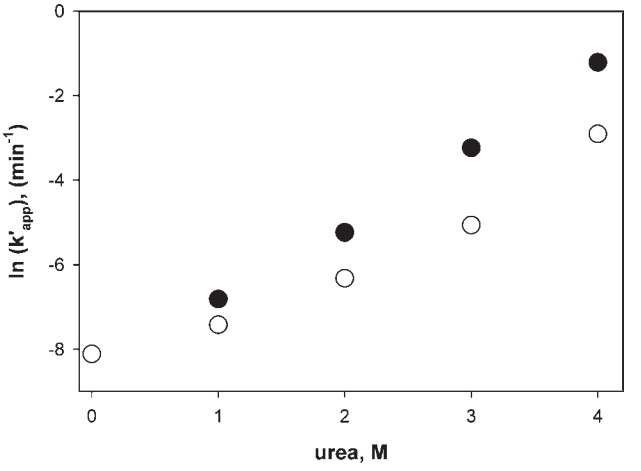

Figure 8. Effects of urea on the reaction rate of the Cys121 thiol with DTNB: (open symbols) palmitate-saturated BLG; (solid symbols) ligand-free BLG.

However, as made evident in Figure 8, in the presence of palmitate the rates of Cys121 exposure were much slower than in the absence of the ligand, and the urea-dependent rate increase was much less pronounced. The palmitate-dependent difference in the reaction rate indeed increased from a factor of ~2 at 1 M urea to a factor of ~8 at 4 M urea.

Structural Aspects and Practical Implications of Ligand-Dependent Stabilization. All of our data concur to indicate that there are several structural regions in BLG, the stability of which

is affected by the binding of palmitate, which was taken here as the epitome of natural ligands in view of our MS characterization of the as-isolated protein. Whereas the protective effect of bound palmitate on the calyx region of the protein where it specifically binds was expected, protection of other structural regions, as recognized by our spectroscopic and analytical approaches, calls for some additional reasoning and may offer some novel insights on the interaction between various structural elements of the protein. Some of the observations reported here may also be of practical relevance in the dairy industry.

The protective effect of bound palmitate with respect to Trp19 at the calyx bottom seems of straightforward interpretation, but the observation that its exposure to the solvent occurs at lower urea concentrations than those required for altering the Trp contribution to the near-UV CD spectrum of the protein may seem puzzling at first. Trp61 on the calyx rim contributes to the CD signal in the near-UV region, and our data suggest that interactions at the rim region are less sensitive to urea than those stabilizing a hydrophobic environment around Trp19 when palmitate occupies the cavity. Our kinetic data also suggest that the stabilizing effect is thermodynamic rather than kinetic in its nature. In conclusion, bound fatty acids (that reportedly bind "tail down" into the calyx[20,31]) make the whole structure of the barrel sensibly tighter, so that it resists chemical and physical denaturants acting both on the main body of the barrel (the actual antiparallel strands) or on its rim. A number of studies have indicated turns and loops at the barrel rim as being responsible for controlling access and release of ligands (see ref 21 and references cited therein).

Changes in thiol reactivity (implying an alteration of the hydrophobic contacts between the calyx exterior and the α-helix regions of the protein, see Figure 1) occur at urea concentrations far below those affecting the two tryptophan residues taken as reporters of structural changes. This region was also reported to be the most sensitive to heat treatments,[6−8] and its modification has been demonstrated to trigger heat- and chaotrope-induced aggregation.[10,14] Because our MS data give no evidence of additional palmitate binding to this region (in accordance with other literature evidence[21,22]), it is the calyx-bound palmitate that makes slower and more difficult the movement of the helix region that exposes Cys121 during limited (and reversible) unfolding.

This implies that palmitate bound to the calyx interior acts on some structural "latch" that stabilizes the closed position of the helix from the outside of the calyx itself. In this frame, the observation that the BLG−palmitate complex has a lower affinity for ANS (a molecule that binds at the hydrophobic patch where the calyx exterior and the hydrophobic side of the helix came close[35]) supports a hydrophobic nature for this hypothetical latch. This hypothesis is corroborated by the results obtained in DSC, which clearly show that the stabilizing effect of the palmitate on the first energetic domain (associated with the helix−barrel interaction) has an entropic nature, as typical of hydrophobic interactions. These modifications precede (and occur independently of) those involving the bottom and the rim of the calyx region, as discussed above.

The practical relevance of our observations may be regarded as self-evident. Aggregation of BLG is a major event in the dairy industry, and its control is of paramount relevance, for instance, in cheesemaking (where formation of BLG aggregates is desirable, but interaction with κ-casein is not, see below) or in milk sanitization treatments (where fouling of heat exchangers represents a problem), or again in what affects the long-term stability of dairy products and/or the accessibility of antigenic or immunoreactive portions of the molecule. It has been long established[36] that thiol groups in BLG are responsible for disulfide exchange events with cysteine residues in other milk proteins, which include the formation of adducts between κ-casein and BLG itself and may impair or prevent the proteolytic events on κ-casein essential to enzymatic curd formation.

Some of these issues have been addressed from a practical standpoint by resorting to the addition of various stabilizing agents or by suggesting alternative treatments. This paper shows that the thermodynamics and kinetics of the molecular events that determine unfolding-dependent aggregation relate to the presence/absence of physiological ligands, an aspect that deserves some deeper understanding and thorough consideration within this particular framework.

■ ASSOCIATED CONTENT

Supporting Information. Figure 1S. This material is available free of charge via the Internet at http://pubs.acs.org.

■ AUTHOR INFORMATION

Corresponding Author

*Phone: +39-02-5031-6819. Fax: +39-02-5031-6801. E-mail: stefania.iametti@unimi.it.

■ ABBREVIATIONS USED

BLG, bovine β-lactoglobulin; ANS, 1,8-anilinonaphthalenesulfonate; ESI-MS, electrospray ionization mass spectrometry; DTNB, 5,5′-dithiobis(2-nitrobenzoic acid); DSC, differential scanning calorimetry.

■ REFERENCES

(1) Hambling, S. G.; Mc Alpine, A.; Sawyer, L. β-Lactoglobulin. In *Milk Proteins*; Fox, P. F., Ed.; Elsevier: London, U.K., 1992; pp 141−190.

(2) Papiz, M. Z.; Sawyer, L.; Eliopoulos, E. E.; North, A. C. T.; Findlay, J. B. C.; Sivaprasadarao, R.; Jones, T. A.; Newcomer, M. E.; Kraulis, P. J. The structure of β-lactoglobulin and its similarity to plasma retinol-binding protein. *Nature* **1986**, *324*, 383–385.

(3) Pervaiz, S.; Brew, K. Homology of β-lactoglobulin, serum retinol-binding protein and protein HC. *Science* **1985**, *228*, 335–337.

(4) Monaco, H. L.; Zanotti, G.; Spadon, P.; Bolognesi, M.; Sawyer, L.; Eliopoulos, E. E. Crystal structure of the trigonal form of bovine β-lactoglobulin and its complex with retinol at 2.5 Å resolution. *J. Mol. Biol.* **1987**, *197*, 695–706.

(5) Brownlow, S.; Morais Cabral, J. H.; Cooper, R.; Flower, D. R.; Yewdall, S. J.; Polikarpov, I.; North, A. C. T.; Sawyer, L. Bovine β-lactoglobulin at 1.8 Å resolution — still an enigmatic lipocalin. *Structure* **1997**, *5*, 481–495.

(6) Iametti, S.; De Gregori, B.; Vecchio, G.; Bonomi, F. Modifications occur at different structural levels during the heat denaturation of β-lactoglobulin. *Eur. J. Biochem.* **1996**, *237*, 106–112.

(7) Iametti, S.; Cairoli, S.; De Gregori, B.; Bonomi, F. Modifications of high-order structures upon heating of β-lactoglobulin − dependence on the protein concentration. *J. Agric. Food Chem.* **1995**, *43*, 53–58.

(8) Fessas, D.; Iametti, S.; Schiraldi, A.; Bonomi, F. Thermal unfolding of monomeric and dimeric β-lactoglobulins. *Eur. J. Biochem.* **2001**, *268*, 5439–5448.

(9) Roefs, S. P. F. M.; De Kruif, K. G. A model for the denaturation and aggregation of β-lactoglobulin. *Eur. J. Biochem.* **1994**, *226*, 883–889.

(10) Rasmussen, P.; Barbiroli, A.; Bonomi, F.; Faoro, F.; Ferranti, P.; Iriti, M.; Picariello, G.; Iametti, S. Formation of structured polymers

upon controlled denaturation of β-lactoglobulin with different chaotropes. *Biopolymers* **2007**, *86*, 57–72.

(11) Iametti, S.; Transidico, P.; Bonomi, F.; Vecchio, G.; Pittia, P.; Rovere, P.; Dall'Aglio, G. F. Molecular modifications of β-lactoglobulin upon exposure to high pressures. *J. Agric. Food Chem.* **1997**, *45*, 23–29.

(12) Belloque, J.; Chicón, R.; López-Fandiño, R. Unfolding and refolding of β-lactoglobulin subjected to high hydrostatic pressure at different pH values and temperatures and its influence on proteolysis. *J. Agric. Food Chem.* **2007**, *55*, 5282–5288.

(13) Cairoli, S.; Iametti, S.; Bonomi, F. Reversible and irreversible modifications of β-lactoglobulin upon heating. *J. Protein Chem.* **1994**, *13*, 347–354.

(14) Iametti, S.; Scaglioni, L.; Mazzini, S.; Vecchio, G.; Bonomi, F. Structural features and reversible association of different quaternary structures of β-lactoglobulin. *J. Agric. Food Chem.* **1998**, *46*, 2159–2166.

(15) Lozinsky, E.; Iametti, S.; Barbiroli, A.; Likhtenshtein, G. I.; Kalai, T.; Hideg, K.; Bonomi, F. Structural features of transiently modified β-lactoglobulin relevant to the stable binding of large hydrophobic molecules. *Protein J.* **2006**, *25*, 1–15.

(16) Iametti, S.; Rasmussen, P.; Frøkiær, H.; Ferranti, P.; Addeo, F.; Bonomi, F. Limited proteolysis of bovine β-lactoglobulin during thermal treatment in sub-denaturing conditions highlights some structural features of the temperature-modified protein and yields fragments with low immunoreactivity. *Eur. J. Biochem.* **2002**, *269*, 1362–1372.

(17) Ragona, L.; Fogolari, F.; Zetta, L.; Perez, D. M.; Puyol, P.; De Kruif, K.; Lohr, F.; Ruterjans, H.; Molinari, H. Bovine β-lactoglobulin: interaction studies with palmitic acid. *Protein Sci.* **2000**, *9*, 1347–135.

(18) Yang, M. C.; Chen, N. C.; Chen, C. J.; Wu, C. Y.; Mao, S. J. Evidence for β-lactoglobulin involvement in vitamin D transport in vivo − role of the γ-turn (Leu-Pro-Met) of β-lactoglobulin in vitamin D binding. *FEBS J.* **2009**, *276*, 2251–2265.

(19) Riihimäki-Lampén, L. H.; Vainio, M. J.; Vahermo, M.; Pohjala, L. L.; Heikura, J. M.; Valkonen, K. H.; Virtanen, V. T.; Yli-Kauhaluoma, J. T.; Vuorela, P. M. The binding of synthetic retinoids to lipocalin β-lactoglobulins. *J. Med. Chem.* **2010**, *14*, 514–518.

(20) Kontopidis, G.; Sawyer, L. The ligand-binding site of bovine β-lactoglobulin: evidence for a function? *J. Mol. Biol.* **2002**, *318*, 1043–1055.

(21) Beringhelli, T.; Eberini, I.; Galliano, M.; Pedoto, A.; Perduca, M.; Sportello, A.; Fontana, E.; Monaco, H. L.; Gianazza, E. pH and ionic strength dependence of protein (un)folding and ligand binding to bovine β-lactoglobulins A and B. *Biochemistry* **2002**, *41*, 15415–15422.

(22) Barbiroli, A.; Beringhelli, T.; Bonomi, F.; Donghi, D.; Ferranti, P.; Galliano, M.; Iametti, S.; Maggioni, D.; Rasmussen, P.; Scanu, S.; Vilardo, M. C. Bovine β-lactoglobulin acts as an acid-resistant drug carrier by exploiting its diverse binding regions. *Biol. Chem.* **2010**, *391*, 21–32.

(23) Ellman, G. L. Tissue sulfhydryl groups. *Arch. Biochem. Biophys.* **1959**, *82*, 70–77.

(24) Pace, C. N. Measuring and increasing protein stability. *Trends Biotechnol.* **1990**, *8*, 93–98.

(25) Barone, G.; Del Vecchio, P.; Fessas, D.; Giancola, C.; Graziano, G. THESEUS: a new software package for the handling and analysis of thermal denaturation data of biological macromolecules. *J. Therm. Anal.* **1992**, *38*, 2779–2790.

(26) Press, W. H.; Flannery, B. P.; Teukolsky, S. A.; Vetterling, W. T. Numerical recipes. In *The Art of Scientific Computing*; Cambridge University Press: Cambridge, U.K., 1989; pp 521−538,

(27) Sanchez-Ruiz, J. M. Theoretical analysis of Lumry−Eyring models in differential scanning calorimetry. *Biophys. J.* **1992**, *61*, 921–935.

(28) Considine, T.; Patel, H. A.; Singh, H.; Creamer, L. K. Influence of binding of sodium dodecyl sulfate, all-trans-retinol, palmitate, and 8-anilino-1-naphthalenesulfonate on the heat-induced unfolding and aggregation of β-lactoglobulin B. *J. Agric. Food Chem.* **2005**, *53*, 3197–3205.

(29) Santambrogio, C.; Grandori, R. Monitoring the Tanford transition in β-lactoglobulin by 8-anilino-1-naphthalene sulfonate and mass spectrometry. *Rapid. Commun. Mass Spectrom.* **2008**, *22*, 4049–4054.

(30) Collini, M.; D'Alfonso, L.; Molinari, H.; Ragona, L.; Catalano, M.; Baldini, G. Competitive binding of fatty acids and the fluorescent probe 1,8-anilinonaphthalene sulfonate to bovine β-lactoglobulin. *Protein Sci.* **2003**, *12*, 1596–1603.

(31) Wu, S. Y.; Pérez, M. D.; Puyol, P.; Sawyer, L. β-Lactoglobulin binds palmitate within its central cavity. *J. Biol. Chem.* **1999**, *274*, 170–174.

(32) Sakurai, K.; Goto, Y. Principal component analysis of the pH-dependent conformational transitions of bovine β-lactoglobulin monitored by heteronuclear NMR. *Proc. Natl. Acad. Sci. U.S.A.* **2007**, *104*, 15346–15351.

(33) Katakura, Y.; Totsuka, M.; Ametani, A.; Kaminogawa, S. Tryptophan-19 of β-lactoglobulin, the only residue completely conserved in the lipocalin superfamily, is not essential for binding retinol, but relevant to stabilizing bound retinol and maintaining its structure. *Biochim. Biophys. Acta* **1994**, *1207*, 58–67.

(34) Greene, L. H.; Chrysina, E. D.; Irons, L. I.; Papageorgiou, A. C.; Acharya, K. R.; Brew, K. Role of conserved residues in structure and stability: tryptophans of human serum retinol-binding protein, a model for the lipocalin superfamily. *Protein Sci.* **2001**, *10*, 2301–2316.

(35) Collini, M.; D'Alfonso, L.; Baldini, G. New insight on β-lactoglobulin binding sites by 1-anilinonaphthalene-8-sulfonate fluorescence decay. *Protein Sci.* **2000**, *9*, 1968–1974.

(36) Sawyer, W. H. Complex between β-lactoglobulin and κ-casein. A review. *J. Dairy Sci.* **1969**, *52*, 1347–1351.

(37) Sayle, R. A.; Milnerwhite, E. J. RASMOL − Biomolecular graphics for all. *Trends Biochem. Sci.* **1995**, *20*, 374–376.